Bond-Slip in Reinforced Concrete Elements

Bibiana María Luccioni[1]; Daniel Ernesto López[2]; and Rodolfo Francisco Danesi[3]

Abstract: A model for fiber reinforced composites that takes into account the fiber slipping is presented in this paper and applied to the analysis of reinforced concrete elements. The model is formulated within the framework of the plasticity theory and the mixtures theory, considering two phases corresponding to the matrix (concrete) and the fibers (reinforcing bars) and modifying the behavior of the last to take into account the relative displacement between the two phases. An elasto-plastic interface model developed by other writers is used to describe the bond–slip mechanism. The resulting model is attractive for the analysis of reinforced concrete problems at the macro-structural level since the explicit discretization of reinforcing bars and interface is not required, with the consequent computational cost reduction. The paper concludes with application examples and comparisons with experimental results of reinforced concrete elements that show the capacity of the model developed.

DOI: XXXX

CE Database subject headings: Concrete, reinforced; Steel; Bonding; Bond stress; Slip; Confinement; Numerical models.

Introduction

When a reinforced concrete structure is progressively loaded, the stresses in the interface between concrete and steel are increased and the capacity of the interface to transmit stress begins to deteriorate at certain load levels. This damage gradually spreads to the surrounding material. With the evolution of this process, the capacity of the interface to transmit stresses is seriously affected and important displacements between steel and concrete can take place.

A great effort has been made in order to understand the main mechanisms of stress transfer between steel and concrete through experimental tests. As a result, reinforced concrete is one of the composite materials for which more experimental information related to the slipping phenomenon is available (Campi et al. 1982; Eligehausen et al. 1983; Gambarova et al. 1989; Malvar 1992; Cox and Yu 1999; Soh et al. 1999).

[1]Civil Engineer, Master in Structural Engineering, Doctor in Engineering, Associate Professor at National Univ. of Tucumán, Researcher of CONICET (National Cientific and Technical Council of Argentina) in Structures Institute, National Univ. of Tucumán, Juan B. Terán 375, 4107 Yerba Buena, Tucumán, Argentina (corresponding author). E-mail: bluccioni@herrera.unt.edu.ar

[2]Civil Engineer, Master in Structural Engineering, Assistant Professor at National Univ. of Cuyo, Research Assistant in Structures Institute, National Univ. of Tucumán, Av. Roca 1800, 4000 S.M. de Tucumán, Argentina. E-mail: dlopez_engadv@yahoo.com.ar

[3]Civil Engineer, Master in Engineering, PhD, Structures Institute Director, Professor at National Univ. of Tucumán, Researcher of CONICET in Structures Institute, National Univ. of Tucumán, Av. Roca 1800, 4000 S.M. de Tucumán, Argentina. E-mail: rdanesi@herrera.unt.edu.ar

Note. Associate Editor: Enrico Spacone. Discussion open until April 1, 2006. Separate discussions must be submitted for individual papers. To extend the closing date by one month, a written request must be filed with the ASCE Managing Editor. The manuscript for this paper was submitted for review and possible publication on October 18, 2002; approved on May 16, 2005. This paper is part of the ***Journal of Structural Engineering***, Vol. 131, No. 11, November 1, 2005. ©ASCE, ISSN 0733-9445/2005/11-1–XXXX/$25.00.

The main stress transfer mechanisms between concrete and steel in reinforced concrete elements are represented by adhesion, mechanical interaction, and friction. Adhesion is constituted by chemical bonds and stresses developed during the curing process of concrete. This transfer mechanism, schematically represented in Fig. 1, is prevailing in the case of bars of smooth surface and its failure is characterized by the initiation and propagation of cracks in the concrete/steel interface.

In the case of corrugated bars, the described mechanism is secondary and the stress transfer is mainly due to the interaction between ribs and the surrounding concrete. Adhesion is relatively soon exhausted in the global response and consequently, the transfer force is transmitted by friction and mechanical interaction between ribs and the adjacent concrete.

As the force in the reinforcing bar is increased, the transfer forces are dominated by the mechanical interaction concentrating at the faces of the ribs. In this state, the term "adhesion stress" refers to the mean force per unit of surface. At increased loading, the concrete begins to fail near the ribs with two different modes of failure; by failure of the concrete adjacent to the contact area, as illustrated in Fig. 2 and by transverse cracking.

Transverse cracking initiates at the ribs presenting a characteristic cone shape, also called secondary cracking or adhesion cracking. The bond zone, constituted by a damaged zone with finite depth surrounding the steel bar, is defined by the extension of the transverse cracking (Fig. 3).

With the stable propagation of transverse cracking, the concrete next to the bar seems to form inclined struts that are known as compression cones (Fig. 4). The adhesion stiffness is usually characterized by the stiffness of these struts.

When the load is further increased, radial splitting forces can be developed. This phenomenon is due to the rotation of the inclined struts (Fig. 4) that produces a considerable radial component of the contact force, the increase of the radial force that is produced by the increase of the effective contact angle between ribs and concrete due to the deposition of the crushed concrete at the faces of the ribs, the wedge action of the ribs, and the radial component of the contact forces. Without an accurate confinement, a splitting failure can occur, spreading the effect of bond outside the bond zone.

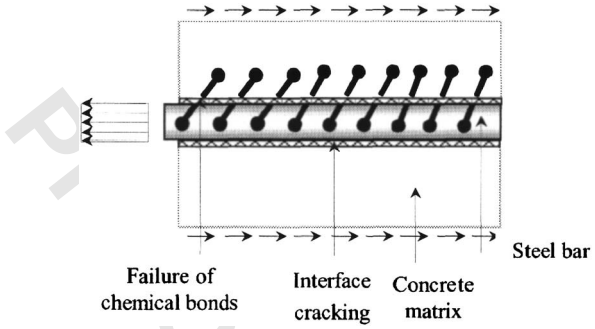

Fig. 1. Schematic representation of adhesion between concrete and steel and its failure

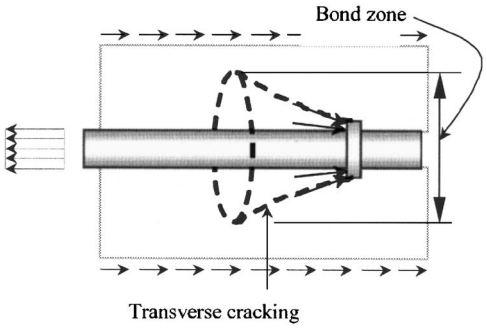

Fig. 3. Stress concentration: transverse cracking

The bond zone dilation, due to the longitudinal cracking, takes place when the adhesion stress reaches values next to the limit one. Following this moment, a stress softening is observed in the response. This stress softening, characteristic of the bond–slip behavior, is frequently interpreted as a progressive shear failure of concrete between the ribs. When the confinement stresses are low, the geometric variation in the contact occurring between the ribs and concrete can also contribute to the stress softening. Both the progressive shear failure of concrete and the contact zone geometric variation are stimulated by the reduction of the confinement stresses produced by the propagation of longitudinal cracking. In both cases, the stress softening reveals a strong discontinuity between the reinforcing bar and the surrounding concrete.

Although the phenomena that govern the stress transfer mechanisms between concrete and steel are developed at the micromechanical scale, they strongly condition and influence the global behavior of the structure, both under service loads and ultimate loads. This situation has been recognized by many researchers like Bresler and Bertero (1968), Takeda et al. (1970), Ma et al. (1976), Ghandehari et al. (1999), Chaboche et al. (1997), and Soh et al. (1999). Experimental tests on reinforced concrete subassemblages have documented the drop of initial structural stiffness due to the reinforcing bar slips above the foundations and in the beam–column connections (Spacone and Limkatanyu 2000).

Many researchers have tried to numerically model the main mechanisms of stress transfer between steel and concrete at different scales. Nevertheless, many of the proposed models that are able to reasonably reproduce the phenomenon encountered present the disadvantage of not being for complete structures analysis due to the elevated computational cost required. Recently, some researchers (Ayoub and Fillippou 1999; Monti and Spacone 2000; Salari and Spacone 2001) have introduced the possibility of slipping and the nonlinearity of the material in the formulation of bar elements. This approach presents advantages over the preceding ones since it does not require the previous determination of the sectional strength–deformation relations and at the same time includes the possibility of discarding the assumption of perfect bond between steel and concrete. Nevertheless, all the models proposed are uniaxial models, strongly dependent on the loading history defining the uniaxial adhesion–displacement relation incorporated into their formulation. Furthermore, they cannot take into account the important and experimentally observed influence of the transverse confinement stresses (Gambarova et al. 1989; Malvar 1992). In view of the limitations of bar elements, other researchers (Pijaudier-Cabot et al. 1991; Cox and Herrmann 1998; Soh et al. 1999; Guo and Cox 2000) have proposed damage models and interface models. These models can overcome the previously mentioned limitations but they have the inconvenience of requiring the explicit discretization of the interface with the consequent additional computational cost involved which may prohibit the analysis of a complete reinforced concrete structure.

One way to reproduce the behavior of reinforced concrete from the constitutive equations of its components and without the explicit discretization of the reinforcing bars is through the application of the mixtures theory. This theory has the limitation assumption of strain compatibility among the different components. This limitation can be overcome through a modification introduced at the bar constitute level (Car 2000). A model for reinforced concrete based on a modification mixtures theory taking into account reinforcement slipping is presented in this paper. A general way to introduce the bond–slip mechanism in the constitutive equation of the reinforcing bars is proposed (Luccioni and López 2002). Within this general framework, local effects belong-

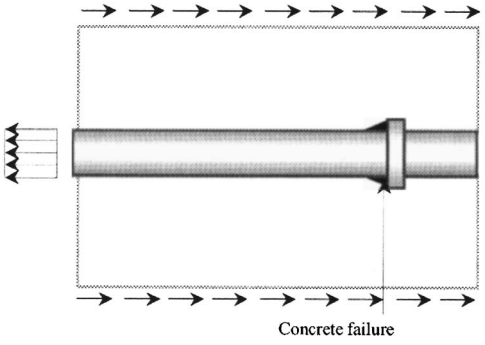

Fig. 2. Failure of concrete in contact with face of rib

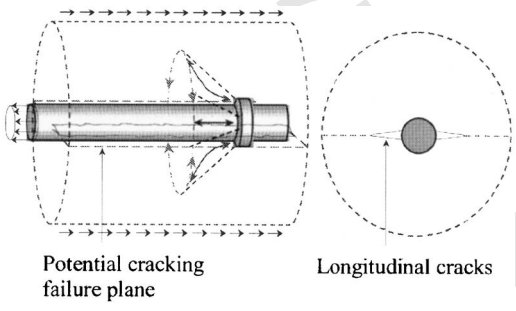

Fig. 4. Change of direction of struts: longitudinal cracking

ing to the scale of the superficial configuration of the bars can be taken into account without using a fine discretization. This fact makes the model particularly attractive for the finite element analysis of macrostructural problems.

Proposed Model

The theory of mixtures is based on the following assumptions (Truesdell and Toupin 1960): (1) the set of component substances is present in each infinitesimal volume of the composite; (2) each component contributes to the behavior of the composite in proportion to its volumetric participation; (3) the volume occupied by each component is lesser than the volume occupied by the composite; and (4) all the components have the same strain (compatibility condition). For small strains, this last assumption is written as

$$\boldsymbol{\varepsilon} = \boldsymbol{\varepsilon}_1 = \boldsymbol{\varepsilon}_2 = \ldots = \boldsymbol{\varepsilon}_n \tag{1}$$

where $\boldsymbol{\varepsilon}$ and $\boldsymbol{\varepsilon}_n$ represent the strain of the composite and of nth component.

The strain compatibility assumption constitutes a strong limitation of the theory of mixtures. In particular, the slipping of reinforcing bars represents a strong discontinuity in the strain field inside the composite that cannot be simulated with this theory. When slipping occurs, the stress transfer between the matrix and the fibers is affected and a stress reduction results in the fibers. This stress reduction can be assimilated to a strain reduction related to the interface deformation (Luccioni and López 2002).

For the case of a composite formed by two components, matrix and fibers, the strain compatibility Eq. (1) can be replaced by the following equation:

$$\boldsymbol{\varepsilon}_f = \boldsymbol{\varepsilon}_m - \boldsymbol{\varepsilon}^s = \boldsymbol{\varepsilon} - \boldsymbol{\varepsilon}^s \tag{2}$$

where subindexes f and m refer to fibers or steel reinforcement and concrete matrix respectively; while $\boldsymbol{\varepsilon}^s$=strain tensor that represents a measure of the interface deformation or slipping. This deformation depends on the stress state and is composed of an elastic component and an irrecoverable component. In general, the elastic component can be neglected when compared with the inelastic deformation, the latter being interpreted as an irrecoverable deformation which takes place as a result of the fiber slipping.

If an elasto-plastic behavior is assumed for steel, the fiber's secant constitutive equation can be written as follows:

$$\boldsymbol{\sigma}_f = \mathbf{C}_f : \boldsymbol{\varepsilon}^e = \mathbf{C}_f : (\boldsymbol{\varepsilon}_f - \boldsymbol{\varepsilon}^p) \tag{3}$$

where $\boldsymbol{\sigma}_f$=reinforcing steel stress tensor; $\boldsymbol{\varepsilon}^e$ and $\boldsymbol{\varepsilon}^p$ represent the elastic and permanent strains, respectively; and $\mathbf{C}_f$=secant constitutive tensor.

Combining Eq. (3) with the strains compatibility Eq. (2) the following equation is obtained:

$$\boldsymbol{\sigma}_f = \mathbf{C}_f : (\boldsymbol{\varepsilon} - \boldsymbol{\varepsilon}^p - \boldsymbol{\varepsilon}^s) \tag{4}$$

Eq. (4) can be used within the framework of theory of mixtures to obtain the stress state in the reinforcing bars from the strain of the composite. For this purpose, it should be assumed that two dissipative mechanisms take place in the set formed by the reinforcing bars together with the interface. One dissipative mechanism is due to the inelastic strains of the steel and the other is due to slipping of the steel bars. Associated with these two mechanisms, two sets of internal variables are defined. The following flow rules are defined for the inelastic strains of the bars and the slipping:

$$\dot{\boldsymbol{\varepsilon}}^p = \dot{\lambda}_p \frac{\partial G_p}{\partial \boldsymbol{\sigma}_f}$$

$$\dot{\mathbf{p}} = \dot{\lambda}_p \mathbf{h}^p \tag{5}$$

$$\dot{\lambda}_p \begin{cases} = 0 \text{ if } F_p(\boldsymbol{\sigma}_f, \mathbf{p}) < 0 \\ > 0 \text{ for } F_p(\boldsymbol{\sigma}_f, \mathbf{p}) = 0 \end{cases} \tag{6}$$

$$\dot{\boldsymbol{\varepsilon}}^s = \dot{\lambda}_s \frac{\partial G_s}{\partial \boldsymbol{\sigma}_f}$$

$$\dot{\mathbf{s}} = \dot{\lambda}_s \mathbf{h}^s \tag{7}$$

$$\dot{\lambda}_s \begin{cases} = 0 \text{ if } F_s(\boldsymbol{\sigma}_f, \mathbf{s}) < 0 \\ > 0 \text{ for } F_s(\boldsymbol{\sigma}_f, \mathbf{s}) = 0 \end{cases} \tag{8}$$

where $\mathbf{p}$ and $\mathbf{s}$ represent sets of internal variables associated with plasticity and slipping mechanisms and $\mathbf{h}^p$ and $\mathbf{h}^s$=tensors defining the flow of each of the internal variables. G_p and G_s represent convex potential functions; $\dot{\lambda}_p$ and $\dot{\lambda}_s$=plastic and slipping consistency parameters; and $F_p(\boldsymbol{\sigma}_f, \mathbf{p}) \leqslant 0$ and $F_s(\boldsymbol{\sigma}_f, \mathbf{s}) \leqslant 0$=plasticity and slipping threshold functions, respectively, which should also be convex functions (Maugin 1992).

The loading/unloading conditions are derived from the Kuhn Tucker's equations and are written as:

$$\text{plasticity: } \begin{cases} \dot{\lambda}_p \geqslant 0 \\ F_p \leqslant 0 \\ \dot{\lambda}_p F_p = 0 \end{cases}$$

$$\text{slipping: } \begin{cases} \dot{\lambda}_s \geqslant 0 \\ F_s \leqslant 0 \\ \dot{\lambda}_s F_s = 0 \end{cases} \tag{9}$$

The model previously defined can be introduced in mixture theory, considering two components: a concrete matrix and the steel fibers or reinforcing bars with bond–slip effect, to simulate the behavior of reinforced concrete. The free energy density per unit of volume of the composite can be written as follows:

$$\Psi(\boldsymbol{\varepsilon}, \mathbf{q}) = k_m \Psi_m(\boldsymbol{\varepsilon}, \mathbf{p}_m) + k_f \Psi_{fs}(\boldsymbol{\varepsilon}^e, \mathbf{p}, \mathbf{s}) \tag{10}$$

where k_m and k_f represent the volume ratios of the concrete matrix and the steel bars respectively; Ψ_m and Ψ_{fs}=free energy densities of the concrete and the steel bars considering the interface; and $\mathbf{p}_m$ represents a set of internal variables of the matrix.

The secant constitutive equation for the composite results

$$\boldsymbol{\sigma} = \frac{\partial \Psi(\boldsymbol{\varepsilon}, \mathbf{q})}{\partial \boldsymbol{\varepsilon}} = k_m \frac{\partial \Psi_m(\boldsymbol{\varepsilon}, \mathbf{p}_m)}{\partial \boldsymbol{\varepsilon}} + k_f \frac{\partial \Psi_{\mathrm{fs}}(\boldsymbol{\varepsilon}^e, \mathbf{p}, \mathbf{s})}{\partial \boldsymbol{\varepsilon}} = k_m \boldsymbol{\sigma}_m + k_f \boldsymbol{\sigma}_f \tag{11}$$

where $\boldsymbol{\sigma}$=stress tensor for reinforced concrete and $\boldsymbol{\sigma}_m$ and $\boldsymbol{\sigma}_f$ represent the stress tensor for the concrete matrix and the reinforcing bars respectively.

Table 1. Parameters for Interface Model

Parameter	Value used
α_e	0.27
α_p	0.45
M	0.42
d_0	$0.38L_e/L_{adh}$
d_1	$0.53L_e/L_{adh}$
d_2	$0.30L_e/L_{adh}$
σ_0	2.25
β	2.7

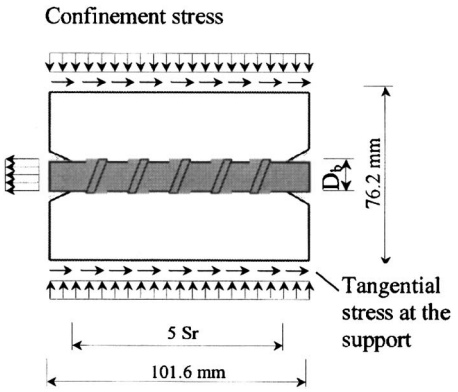

Fig. 5. Schematic representation of Malvar's tests—(68° ribs)

Elasto-Plastic Model for Interface

The elasto-plastic interface model developed by Cox and Hermann (1998) is used to simulate the slipping effect. The original model was modified in order to make it suitable to be included in the composite model described in the paper for a finite element analysis. The main changes were the definition of a strain due to slipping and the definition of the hardening variable in order to ensure objectivity in the softening response when the model is used in combination with the finite element method. Most of the constant parameters were recalibrated based on experimental results.

The model relates the average local displacement and the radial dilatation with the average tangential adhesion stress and the radial confinement stress. The components of the model have been empirically obtained and qualitatively reflect the kinematic of the mechanical interaction between the ribbed steel bars and the surrounding concrete for monotonic loading, as previously described. The model is based on the following assumptions:

- The tangential stresses are uniformly distributed at the interface and
- The slipping is concentrated at the interface.

Additionally, the following simplifying assumptions are considered in this work: the elastic deformation of the interface is neglected and the interface deformation orientation is assumed to correspond to the direction of the bars.

A measure of the length of the adhesion zone d is chosen as an internal variable of the interface. This length cannot exceed the distance between ribs, S_r, since for higher values the interaction between concrete and steel is purely frictional and the yield surface does not evolve. This internal variable d represents a measure of the interface damage and is defined as follows:

$$d = \min[(\delta_t^d/S_r), 1] = \min[(\varepsilon_t^s/S_r)L_{adh}, 1] \tag{12}$$

where min=minimum function; δ_t^d=relative displacement between steel and concrete in the longitudinal direction of the bar; L_{adh}=adhesion length; and ε_t^s=strain component due to the slipping in the longitudinal direction of the bar

$$\varepsilon_t^s = \delta_t^d/L_{adh} = \mathbf{a}_t^T \cdot \boldsymbol{\varepsilon}^s \cdot \mathbf{a}_t \tag{13}$$

$\mathbf{a}_t$ represents a unit vector in the longitudinal direction of the bars.

In order to achieve objectivity of the softening response with respect to the size of the finite element mesh, a characteristic length is included in the model and the hardening variable is defined as follows:

$$d^* = d(L_e/L_{adh}) \tag{14}$$

where L_e=characteristic length that represents the length of the finite element in the longitudinal direction of the steel bar.

The slipping threshold function is described through the function of Eq. (15) that transits between two types of functions: potential and exponential. The change in the slipping threshold function reflects the change in the dominating mode of failure. For low values of damage, the inelastic behavior is mainly due to the mechanical interaction of the ribs. For relatively high values of damage, friction becomes important in the behavior and most of the slipping is due to a strong discontinuity in the displacement field between concrete and steel bars

Table 2. Mechanical Properties of Concrete and Steel [adapted from Malvar (1992)]

Elasticity modulus (MPa)	Poisson coefficient	Compression elastic threshold (MPa)	Compression/tension elastic thresholds ratio	Yielding criteria	Plastic flow
(a) Concrete					
3.724×10^4	0.20	34.32	10	Mohr Coulomb	Associate
(b) Steel					
2.058×10^5	0.20	412.00	1	Von Mises	Fiber
(c) Interface					
D_b (mm)	S_r (mm)	L_{adh} (mm)			
20	12.2	61			

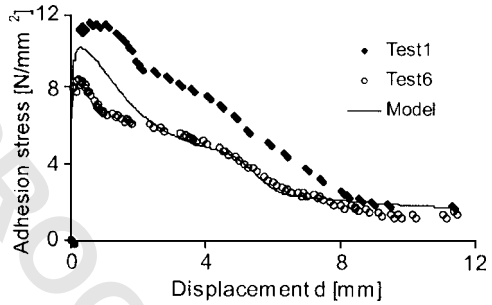

Fig. 6. Tests 1 and 6 (confinement pressure: 3.45 MPa)

$$F_s(\boldsymbol{\sigma}_f, d^*) = |\tau/f_t| - C(d^*)W_e(d^*) + \{1 - \exp[-\alpha_e(-\sigma^n/f_t + \hat{\sigma}(d^*))]\} - C(d^*)M(1 - W_e(d^*))|-\sigma^n/f_t + \hat{\sigma}(d^*)|^{\alpha_p} \times \text{sign}[-\sigma^n/f_t + \hat{\sigma}(d^*)] = 0 \quad (15)$$

exp=exponential function; $\exp x = e^x$, e base of natural logarithms; $e=2.71828$; sign=sign function; and f_t=concrete uniaxial tension strength. M, α_e, and α_p are supposed to be constant. These values were obtained from calibration tests with experimental results (Malvar 1992) and are presented in Table 1. σ^t=longitudinal stress of the steel bars and σ^n=transversal confinement stress

$$\sigma^t = \mathbf{a}_t^T \cdot \boldsymbol{\sigma}_f \cdot \mathbf{a}_t \quad (16)$$

$$\sigma^n = \mathbf{a}_n^T \cdot \boldsymbol{\sigma}_f \cdot \mathbf{a}_n \quad (17)$$

where $\mathbf{a}_n$=unit vector in the direction transversal to the bars.

τ is the adhesion stress defined as

$$\tau = \sigma^t D_b/(4L_{\text{adh}}) \quad (18)$$

D_b=reinforcing bar diameter and $W_e(d^*)$=weight function or transition function defined as

$$W_e(d^*) = \begin{cases} 0 & d^* \in [0, d_0] \\ 3[(d^* - d_0)/(d_1 - d_0)]^2 - 2[(d^* - d_0)/(d_1 - d_0)]^3 & d^* \in (d_0, d_1) \\ 1 & d^* \in [d_1, 1] \end{cases} \quad (19)$$

$$W_e(d^*) \in C^1[0,1]$$

The limits of the interval (d_0, d_1) obtained by calibration with experimental results (Malvar 1992) are defined in Table 1 taking into account the definition of the hardening variable.

$\hat{\sigma}(d^*)$=kinematic strain softening function mainly associated with the geometrical dilation. This function is defined in order to capture the brittle nature of the adhesion mechanism that dominates the behavior for low confinement pressures

$$\hat{\sigma}(d^*) = \begin{cases} \hat{\sigma}_0[(d_2 - d^*)/d_2]^\beta & d^* \in [0, d_2] \\ 0 \quad d^* \in [d_2, 1] \end{cases} \quad (20)$$

where d_2 represents the ending of the kinematic strain softening threshold and its value is presented in Table 1. $\beta > 1$=calibration constant. The value used for β in the present paper was obtained by calibration with experimental results (Cox and Yu 1999) and is presented in Table 1.

$\hat{\sigma}_0$=parameter that defines the magnitude of the kinematic strain softening. The value obtained from the analysis of a thin walled cylinder the value of Cox and Yu (1999) is presented in Table 1. $C(d^*)$ is obtained adjusting experimental results and represents the isotropic strain hardening (Cox and Yu 1999)

$$C(d^*) = -3.30e^{-10(d^*)^{3/5}} + 6.00e^{-2.6(d^*)^{6/5}} + 1.70 \quad (21)$$

The flow rule is written as follows (Luccioni and López 2002):

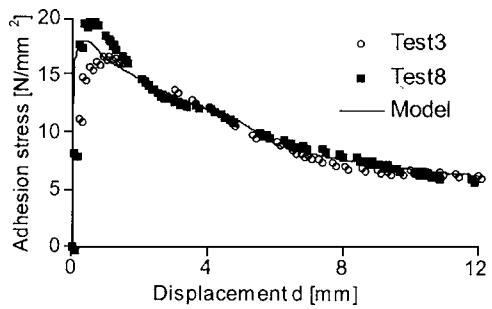

Fig. 7. Tests 3 and 8 (confinement pressure: 17.24 MPa)

Fig. 8. Tests 4 and 9 (confinement pressure: 24.14 MPa)

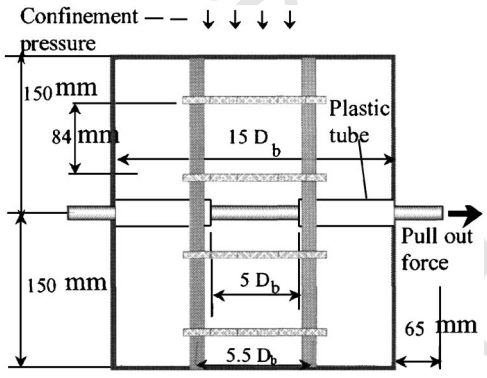

Fig. 9. Schematic representation of Eligehausen's tests

Table 3. Mechanical Properties of Concrete and Steel [adapted from Eligehausen et al. (1983)]

Elasticity modulus (MPa)	Poisson coefficient	Compression elastic threshold (MPa)	Compression/tension elastic thresholds ratio	Yielding criteria	Plastic flow
(a) Concrete					
3.43×10^4	0.20	30.0	10	Mohr Coulomb	Associate
(b) Principal and secondary steel					
2.058×10^5	0.20	412.0	1	Von Mises	Fiber
(c) Interface					
D_b(mm)	S_r(mm)	L_{adh} (mm)			
(c1) Principal steel					
25.4	12.2	127			
(c2) Secondary steel					
12.4	12.2	127			

$$\dot{\boldsymbol{\varepsilon}}^s = \dot{\lambda}_s \frac{\partial G_s}{\partial \boldsymbol{\sigma}_f} = \mathbf{a}_t \cdot \mathbf{a}_t^T \dot{\varepsilon}_t^s \tag{22}$$

Application Examples

Malvar's Tests (Malvar 1992)

In this section the pullout tests performed by Malvar (1992) are simulated using a coarse element mesh. Malvar performed extraction tests with strain control from cylindrical concrete specimens with constant confinement stress and different surface patterns of the steel bars. The main geometrical characteristics of the specimens tested are presented in Fig. 5.

The numerical simulation of the tests is made with one plane stress finite element with four nodes and two integration points in each direction. So coarse mesh can be used because the bond–slip phenomenon is implicitly included in the constitutive equation of the bar that is introduced in the theory of mixtures to consider concrete and steel as a composite considering the properties of each material and the interface.

Concrete is modeled as an elasto-plastic material and the model presented in this paper is used for the steel and interface. The main mechanical properties of the materials are presented in Table 2.

The curves obtained with the model for the mean adhesion stress–displacement relationship for different values of the confinement pressure and their comparison with experimental results (Malvar 1992) are presented in Figs. 6–8. The numerical results show good agreement with the experimental ones even though a coarse finite element meshed was used.

Eligehausen's Tests (Eligehausen et al. 1983)

The results obtained with the model presented are compared with experimental results by Eligehausen et al. (1983) for the adhesion stress–slipping relation (Fig. 9).

One element of a composite material formed by concrete and the horizontal steel bar is used to model the test. The main mechanical properties of the materials are resumed in Table 3.

The adhesion stress–slipping curve obtained is compared with the curve by Eligehausen for unconfined concrete. The model response is close to experimental results although it has been calibrated with results of other experimental series. The response of the model is more brittle than the experimental curves for confined concrete (Eligenhausen et al. 1983). The difference is due to the confinement effect of secondary reinforcement that results in a ductility and strength increment. This effect cannot be modeled with only one finite element (see Fig. 10).

Reinforced Concrete Column with Bar Slipping

The analysis of a reinforced concrete column anchored in a concrete prism and subjected to controlled horizontal displacements at its free end, according to Low and Moehle (1987) tests, is presented in this section (Fig. 11). First, the case of perfect an-

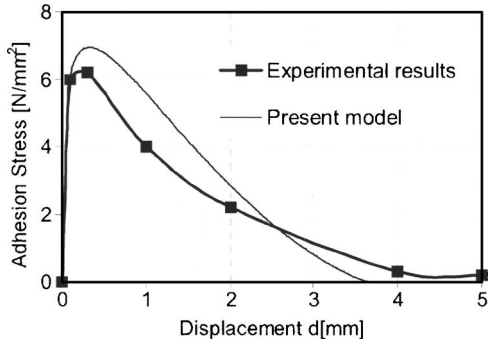

Fig. 10. Comparison with experimental results by Eligehausen et al.

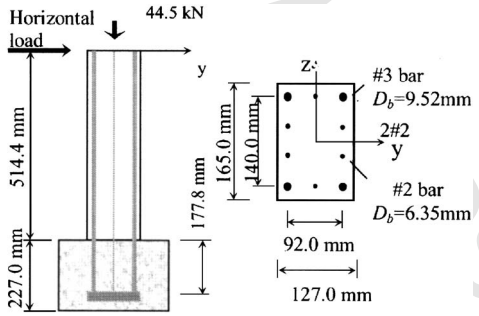

Fig. 11. Schematic representation of Low and Moehle's tests

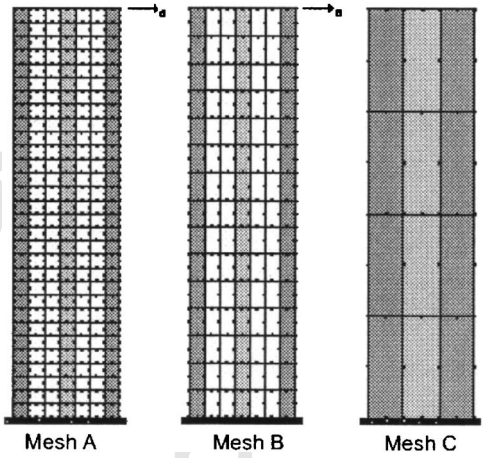

Fig. 12. Finite element meshes

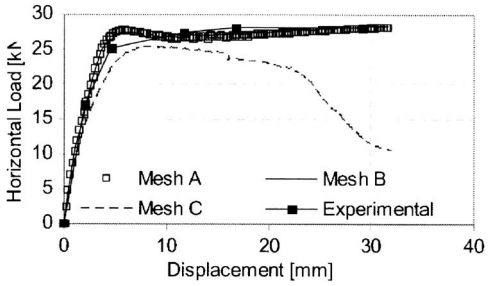

Fig. 13. Load–displacement curve for perfect anchorage

chorage is simulated and the results are compared with experimental ones (Low and Moehle 1987).

Then, the same problem with different anchorage lengths is analyzed allowing slipping of the reinforcement bars. The results are compared with numerical results by Spacone and Limkatanyu (2000).

The numerical results by Spacone and Limkatanyu (2000) were obtained with a reinforced concrete beam finite element that explicitly accounts for the slip between the reinforcing bars and the surrounding concrete. The reinforced concrete beam element is made of a two-node concrete beam and n two-node bars that can slip with respect to the concrete. The nodal degrees of freedom of concrete beam and of the reinforcing bars are different to allow slip. The plane section is assumed to remain plane in the concrete beam formulation. The Kent and Park (1971) law is used for concrete assuming linear elastic behavior in tension up to cracking stress and rapid linear stress degradation for increasing tensile strains. The Menegotto and Pinto's (1973) law is used for steel reinforcing bars. The relative slips between concrete beam and steel bars are related to the bond stresses with the Eligehausen et al. (1983) law for confined concrete.

The numerical simulation using the model presented in this paper is performed with three different meshes (Fig. 12) in order to prove the objectivity of the results with respect to the element size. In all cases, plane stress elements with eight nodes and two integration points in each direction are used. Reinforced concrete (in gray) is modeled as a composite material with different volume ratios of concrete and steel.

The mechanical properties of concrete, steel and the interface are resumed in Table 4.

All the models are first subjected to a vertical compression load of 44.5 kN. Then a controlled monotonically increasing horizontal displacement, in the global direction y, is applied at the free end of the column.

Fig. 13 shows the results obtained for the case of perfect anchorage of the reinforcing bars and the comparison with experimental results (Low and Moehle 1987). A good agreement is achieved between numerical and experimental results for the finer meshes. The differences among the results of Meshes A and B are due to discretization errors of the finite element method (Zienkiewicz and Taylor 2000). It is clear that numerical results converge to experimental ones as the mesh is refined. Mesh C is too coarse, principal reinforcement is spread in a too wide zone and this fact alters the maximum strength.

The results obtained for Meshes A and B allowing slipping of the reinforcement and different anchorage lengths are presented in Fig. 14 and compared with those numerically obtained by Spacone and Limkatanyu (2000) with a fiber element.

In general, the results present a good agreement with those numerically obtained by Spacone and Limkatanyu (2000). The curves by Spacone and Limkatanyu (2000) present the same appearance as the envelope of Eligehausen et al. (1983) on which their bond–slip model is based. Comparison of the results obtained for the two finite element meshes analyzed show that the softening response is objective with respect to the size of the finite elements.

Table 4. Mechanical Properties of Concrete and Steel [adapted from Low and Moehle (1987)]

Elasticity modulus (MPa)	Poisson coefficient	Compression elastic threshold (MPa)	Compression/tension elastic thresholds ratio	Yielding criteria	Plastic flow
(a) Concrete					
2.20×10^4	0.20	36.5	10	Mohr Coulomb	Associate
(b) Steel					
2.058×10^5	0.20	440.0	1	Von Mises	Fiber
(c) Interface					
D_b (mm)	S_r (mm)	L_{adh} (mm)			
9.52	12.2	127.0–76.2–25.4			
6.35	12.2	127.0–76.2–25.4			

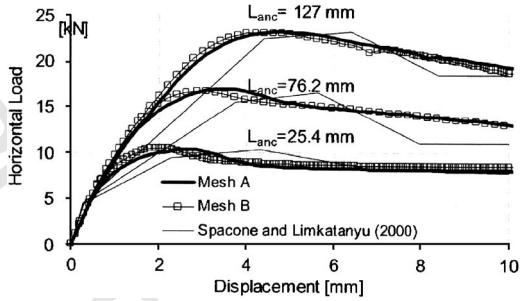

Fig. 14. Load–displacement curve for different anchorage lengths

Conclusions

The model presented in this paper for reinforced concrete allows the slipping of the reinforcing bars without requiring the explicit discretization of the reinforcing bars and the steel/concrete interface. This fact makes it attractive for numerical simulation of concrete structures at the macrostructural level.

In addition to the satisfactory simulation of uniaxial processes, the proposed model can take into account many facts that cannot be simulated by uniaxial models like the effect of confinement pressure, the surface pattern of the reinforcing bars, the dilation of the adhesion zone and the associated cracking.

With respect to other models that do not require the explicit discretization of the interface, the proposed model has the advantage of capturing the influence of the confinement pressure independently from other damage or plastic processes that can take place in the concrete matrix.

The application examples and comparisons with experimental results presented show the ability of the model to reproduce numerical and experimental results from different researchers.

Acknowledgments

The financial support of CONICET and National University of Tucumán is gratefully acknowledged. Special acknowledgement is extended to Ms. Amelia Campos for the English revision.

Notation

The following symbols are used in this paper:

$\mathbf{a}_n$ = unit vector in direction transversal to bars;
$\mathbf{a}_t$ = unit vector in longitudinal direction of bars;
$\mathbf{C}_f$ = secant constitutive tensor of steel fibers;
$C(d^*)$ = isotropic strain hardening function;
D_b = bar diameter;
d = internal variable of interface that represents measure of length of adhesion zone;
d^* = hardening variable for bond–slip mechanism;
d_0 = calibration parameter;
d_1 = calibration parameter;
d_2 = ending of kinematic strain softening threshold;
e = base of natural logarithms, e=2.71828;
F_p = plasticity threshold function;
F_s = slipping threshold function;
f_t = concrete uniaxial tension strength;
G_p = plasticity potential function;
G_s = slipping potential function;
k_f = volume ratio of steel bars;
k_m = volume ratio of concrete matrix;
L_{adh} = adhesion length;
L_e = characteristic length that represents length of finite element in longitudinal direction of steel bar;
M = calibration parameter;
$\mathbf{p}$ = set of internal variables associated with plastic process;
$\mathbf{p}_m$ = set of matrix internal variables;
$\mathbf{q}$ = set of internal variables of composite;
S_r = separation between ribs;
$\mathbf{s}$ = set of internal variables associated with slipping process;
$W_e(d^*)$ = weight function or transition function;
α_e = calibration constant;
α_p = calibration constant;
β = calibration constant;
δ_t^d = relative displacement between steel and concrete in longitudinal direction of bar;
$\boldsymbol{\varepsilon}$ = composite strain tensor;
$\boldsymbol{\varepsilon}^e$ = fibers elastic strains;
$\boldsymbol{\varepsilon}_f$ = fibers strain tensor;
$\boldsymbol{\varepsilon}_m$ = matrix strain tensor;
$\boldsymbol{\varepsilon}_n$ = strain tensor of nth component;
$\boldsymbol{\varepsilon}^p$ = fibers permanent strains;
$\boldsymbol{\varepsilon}^s$ = tensor that represents measure of interface deformation;
ε_t^s = strain component due to slip in longitudinal direction of bar;
λ_p = plastic consistency parameter;
λ_s = slipping consistency parameter;
$\boldsymbol{\sigma}$ = composite stress tensor;
$\boldsymbol{\sigma}_f$ = fibers stress tensor;
$\boldsymbol{\sigma}_m$ = matrix stress tensor;
σ^n = transversal confinement stress;
σ^t = longitudinal stress of steel bars;
$\hat{\sigma}_0$ = parameter that defines magnitude of cinematic strain softening;
$\hat{\sigma}(d^*)$ = kinematic strain softening function mainly associated with geometrical dilation;
$\tau_{\cdot}$ = adhesion stress;
Ψ_{fs} = free energy densities of steel bars considering interface; and
Ψ_m = free energy densities of concrete matrix.

Subscripts

adh = adhesion;
b = bar;
e = elastic;
f = fibers;
m = matrix;
n = transversal;
p = plastic;
r = rib;
s = slipping; and
t = longitudinal.

References

Ayoub, A., and Fillippou, F. (1999). "Mixed formulation of bond-slip problems under cyclic loads." *J. Struct. Eng.*, 125(6), 661–671.

PROOF COPY [ST/2002/023537] 007511QST

Bresler, B., and Bertero, V. (1968). "Behavior of reinforced concrete under repeated load." *J. Struct. Div. ASCE*, 94(6), 1567–1590.

Campi, V., Eligehausen, R., Bertero, V., and Popov, E. (1982). "Analytical model for concrete anchorages of reinforcing bars under generalized excitations." *Rep. No. UCB/EERC-82/23*, Earthquake Engineering Research Center, College of Engineering Univ.

Car, E. (2000). "Modelo constitutivo continuo para el estudio del comportamiento mecánico de los materiales compuestos." PhD thesis, Univ. Politécnica de Cataluña, Spain.

Chaboche, J. L., Girard, R., and Schaff, A. (1997). "Numerical analysis of composite systems by using interphase/interphace models." *Comput. Mech.*, 20, 3–11.

Cox, J. V., and Herrmann, L. (1998). "Development of a plasticity bond model for steel reinforcement." *Mech. Cohesive-Frict. Mater.*, 3, 155–180.

Cox, J. V., and Yu, H. (1999). "A micromechanical analysis of the radial clastic response associated with slender reinforcing elements within a matrix." *J. Compos. Mater.*, 33(23), 16–26.

Eligehausen, R., Bertero, V., and Popov, E. P. (1983). "Local bond-slip relationships of deformed bars under generalized excitations." *Rep. No UCB/EERC 83-19*, Earthquake Engineering Research Center, Univ. of California, Berkeley, Calif.

Gambarova, P. G., Rosati, G. P., and Zasso, B. (1989). "Steel-to-concrete bond after concrete splitting test results." *Mater. Struct.*, 22(127), 35–47.

Ghandehari, M., Krishnaswamy, S., and Shah, S. (1999). "Technique for evaluating kinematics between rebar and concrete." *J. Eng. Mech.*, 125(2), 234–241.

Guo, J., and Cox, J. V. (2000). "An interfacial model for the mechanical interaction between frp bars and concrete." *J. Reinf. Plast. Compos.*, 19(1), 15–34.

Kent, D. C., and Park, R. (1971). "Flexural members with confined concrete." *J. Struct. Div. ASCE*, 97(7), 1969–1990.

Low, S. S., and Moehle, J. P. (1987). "Experimental study of reinforced concrete columns subjected to multi-axial cyclic loading." *EERC Rep. No. 87/14*, Earthquake Engineering Research Center, Univ. of California, Berkely, Calif.

Luccioni, B., and López, D. (2002). "Modelo para materiales compuestos con deslizamiento de fibras." *Análisis y cálculo de estructuras de materiales compuestos*, S. Oller, ed., CIME, Barcelona, Spain, 411–431.

Ma, S. Y., Bertero V., and Popov, E. P. (1976). "Experimental and analytical studies on the hysteretic behavior of reinforced concrete rectangular and t-beams." *Rep. No. EERC 79-22*, Earthquake Engrineering Research Center, Univ. of California, Berkeley, Calif.

Malvar, L. J. (1992). "Bond of reinforcement under controlled confinement." *ACI Mater. J.*, 89(6), 593–601.

Maugin, G. A. (1992). *The thermomechanics of plasticity and fracture*, Cambridge University Press, Cambridge, U.K.

Menegotto, M., and Pinto, P. E. (1973). "Method of analysis for cyclically loaded reinforced concrete plane frames including changes in geometry and inelastic behavior of elements under combined normal force and bending." *Final Rep., Proc., IABSE Symp. on Resistance and Ultimate Deformability of Structures Acted on Well Defined Repeated Loads*, Lisboa, Portugal.

Monti, G., and Spacone, E. (2000). "Reinforced concrete fiber beam with bond-slip." *J. Struct. Eng.*, 126(6), 654–661.

Pijaudier-Cabot, G., Mazars, J., and Pulikowski, J. (1991). "Steel-concrete bond analysis with nonlocal continuous damage." *J. Struct. Eng.*, 117(3), 862–882.

Salari, M., and Spacone, E. (2001). "Finite element formulation of one-dimensional elements with bond-slip." *Eng. Struct.*, 23, 815–826.

Soh, C., Chiew, S. P., and Dong, Y. X. (1999). "Damage model for concrete-steel interface." *J. Struct. Eng.*, 125(8), 979–983.

Spacone, E., and Limkatanyu, S. (2000). "Response of reinforced concrete members including bond-slip effects." *ACI Struct. J.*, 97(6), 831–839.

Takeda, T., Sozen, M. and Nielsen, N. N. (1970). "Reinforced concrete response to simulated earthquake." *J. Struct. Div. ASCE*, 96(12), 2557–2573.

Truesdell, C., and Toupin, R. (1960). *The classical field theories, Handbuch der Physik II/I*, S. Flugge, ed., Springer, Berlin.

Zienkiewicz, O. C., and Taylor, R. L. (2000). *Finite element method: Volume 1, The basis*, 5th Ed., Butterworth Heinemann—CIMNE (International Center for Numerical Methods in Engineering), Barcelona, Spain.

PROOF COPY [ST/2002/023537] 007511QST